PHYSICAL REVIEW B VOLUME 62, NUMBER 3 15 JULY 2000-I

Dielectric response of the charge-induced correlated state in the quasi-one-dimensional conductor $(\mathrm{TMTTF})_2\mathrm{PF}_6$

F. Nad,[1,2] P. Monceau,[1] C. Carcel,[3] and J. M. Fabre[3]
[1]Centre de Recherches sur les Très Basses Températures, Laboratoire associé à l'Université Joseph Fourier, CNRS, Boîte Postale 166, 38042 Grenoble cedex 9, France
[2]Institute of Radioengineering and Electronics, Russian Academy of Sciences, Mokhovaya 11, 103907 Moscow, Russia
[3]Laboratoire de Chimie Structurale Organique, Université de Montpellier, 34095 Montpellier cedex 5, France

(Received 13 January 2000)

Conductivity and permittivity of the quasi-one-dimensionsional organic transfer salt $(\mathrm{TMTTF})_2\mathrm{PF}_6$ have been measured at low frequencies (10^3–10^7 Hz) between room temperature down to below the temperature of transition into the spin-Peierls state. We interpret the huge real part of the dielectric permittivity (up to 10^6) in the localized state as the realization in this compound of a charge ordered state of Wigner crystal type due to long-range Coulomb interaction.

I. INTRODUCTION

Conductors formed of linear chains of organic molecules tetramethyltetrathiafulvalene (TMTTF) or tetramethyltetraselenafulvalene (TMTSF) with a general formula $(\mathrm{TMTCF})_2\mathrm{X}$ with C= Se, S, and X and the interchain counterion $=\mathrm{ClO}_4$, PF_6, Br, ... have been intensively studied these last years because they exhibit a rich variety of cooperative phenomena including superconductivity, antiferromagnetism, spin-density wave (SDW), spin-Peierls state, and charge localization.[1] While the Bechgaard $(\mathrm{TMTSF})_2\mathrm{X}$ salts display a metallic behavior down to low temperature where a transition in a SDW state occurs below ~12 K, $(\mathrm{TMTTF})_2\mathrm{X}$ salts exhibit a charge localization in the temperature range of 100–200 K, with a maximum in conductivity at T_ρ and a thermally activated variation below T_ρ,[2,3] revealing strong Coulomb interaction effects in these sulfur salts.

Quasi-one-dimensional conductor $(\mathrm{TMTTF})_2\mathrm{X}$ consists of molecular chains (along the highest conductivity axis) with two electrons per four molecules, which corresponds to 1/4-filling in terms of holes. These molecular chains are slightly dimerized due to intermolecular interaction. As a result, with decreasing temperature a dimerized gap $\Delta\rho$ opens with effective 1/2-filling of the upper conduction band. Two intermolecular transfer integrals along molecular stacks t_1 and t_2 have to be considered.[4] Quantum chemistry calculations show that in $(\mathrm{TMTTF})_2\mathrm{PF}_6$ the dimerization decreases with decreasing temperature and at low temperatures the t_1/t_2 ratio is about 1.1–1.2.[4]

As was shown in several of theoretical and experimental works, between many factors that determine the properties of $(\mathrm{TMTTF})_2\mathrm{X}$-type salts, electron-electron correlation phenomena play the leading part.[1,4–13] In this context two types of theoretical models have been essentially developed. In the frame of the so-called g-ology models,[8,10,14] the electron-electron correlations are considered as a perturbation to the one-electron approach. These models have been used for describing the low-energy properties of these salts that exhibit the features of a Luttinger liquid rather than a Fermi liquid.[14]

The second group of models includes the various versions of the Hubbard model.[9–13,15] The extended Hubbard model takes into account the interaction between charge carriers on the site of host lattice (on-site interaction) with characteristic energy U as well as the interaction between charge carriers on the neighboring sites (near-neighbor interaction) with characteristic energy V. In the case of $(\mathrm{TMTTF})_2\mathrm{X}$ compounds, at temperatures above the transition into spin ordered states, the electron-electron interaction is determined by long-range Coulomb interaction and it is stronger than spin interaction. This is one of the reasons spin-charge separation is one-dimensional observed in such (1D) conductors.[1] In the frame of the extended Hubbard model it was shown that the dimerized energy gap is strengthened taking into account the on-site and near-neighbor interactions.[9] At the same time the spectrum of spin excitations remains gapless, which also corresponds to spin-charge separation.

One important result of the extended Hubbard model approach concerns the formation of a $4k_F$ (CDW) superlattice of Wigner crystal type in such 1D compounds with decreasing temperature. Using the Monte Carlo technique it was shown that, for large enough U and V magnitudes, strictly on-site interaction results only in a weak $4k_F$ CDW, while long-range Coulomb near-neighbor interaction can produce a CDW singularity at $4k_F$.[9] Analogously, using mean-field approximation,[13] it was recently shown that for a one-dimensional molecular chain with and without dimerization the form of the developed superstructure depends considerably on the magnitude of near-neighbor interaction V: at V above some critical value V_c a $4k_F$ CDW superstructure occurs with charge disproportionation depending on V. Estimations of V/U and V/t_2 magnitudes in $(\mathrm{TMTTF})_2\mathrm{PF}_6$, obtained from quantum chemistry calculations and from optical conductivity,[4,12] yields values for V/U in the range 0.4–0.5 and for V/t_2 in the range of 2–3 manifesting the essential role played by the long-range Coulomb interaction in this compound. Hereafter we present results of conductivity and dielectric permittivity measurements of $(\mathrm{TMTTF})_2\mathrm{PF}_6$, which provide some evidence of a charge modulated state (analogous to a Wigner crystal) resulting from electron-electron charge correlation below T_ρ.

0163-1829/2000/62(3)/1753(4)/$15.00

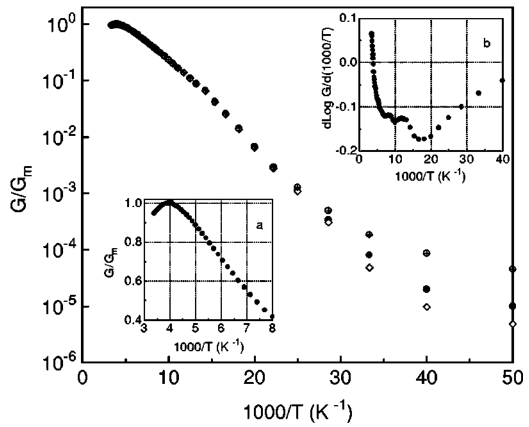

FIG. 1. Variation of the real part of the conductance G (sample 1) normalized to its maximum G_m as a function of the inverse temperature at frequencies (in kHz): ◇ 10, ● 100, and ⊕ 1000. Inset (a) details of the temperature dependence of G/G_m near the maximum. Inset (b) temperature dependence of the logarithmic derivative $d \log G/d(1000/T)$.

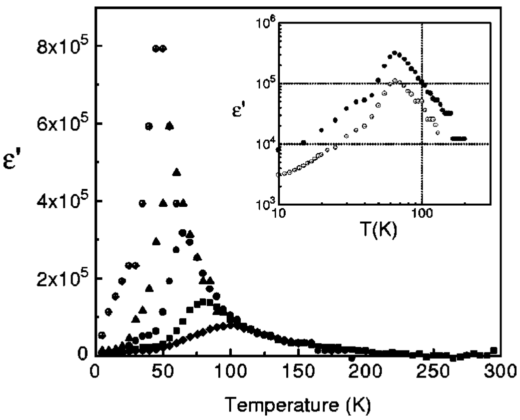

FIG. 2. Temperature dependence of the real part of the dielectric permittivity ϵ' (sample 1) at frequencies (in kHz): ⊕1, ▲10, ●100, ■1000, and ◆5000. Inset: temperature dependence of ϵ' for sample 1 (●) and sample 2 (⊙) at 100 kHz in a double-logarithmic scale.

II. EXPERIMENT

We have studied $(\mathrm{TMTTF})_2\mathrm{PF}_6$ samples originating from two batches. The crystals have been prepared using standard electrochemical procedures.[16] Electrical contacts were prepared by first evaporating gold pads on nearly the whole surface of the sample's ends on which thin gold wires were attached afterwards with silver paste. We have carried out the measurements of complex conductance $G(T,\omega)$, using an impedance analyzer HP 4192A in the frequency range 10^3–10^7 Hz and in the temperature range 4.2–295 K. The amplitude of the ac voltage applied to the sample was within the linear response and typically 30 mV/cm. We have noticed that the cooling rate had a significant effect on the results of our measurements, much more important than in the case of $(\mathrm{TMTTF})_2\mathrm{Br}$ for instance:[17] at a cooling rate above 0.5 K/mm, cracks appear as seen in jumps in the temperature variation of G. However with a slow cooling rate around 0.2 K/mm and along temperature stabilization before performing measurements, we succeeded in recording the temperature dependencies of real and imaginary parts of G without any jumps for three samples. These samples have a length of 3–4 mm, a cross section of about $2\times10^{-5}-10^{-4}\ \mathrm{cm}^2$, and a room-temperature conductivity $\sim 40\ \Omega^{-1}\,\mathrm{cm}^{-1}$. The results obtained for these three samples are qualitatively similar and we will present the data for two of them (referred as samples 1 and 2).

Figure 1 shows the variation of the conductance $G(T)$ of sample 1 normalized by its maximum value G_m as a function of the inverse temperature. The detailed $G(T)$ dependence near the room temperature is shown in inset (a) of Fig. 1. With decreasing temperature, the conductance of $(\mathrm{TMTTF})_2\mathrm{PF}_6$ first grows up to a maximum at $T_\rho = 250$ K as previously reported in Refs. 2 and 3. Below T_ρ, the decrease of $G(T)$ in the temperature range 200–70 K follows an Arrhenius-type behavior with an activation energy $\Delta\rho \simeq 300$ K. The value of this activation energy is in good agreement with the evaluation of the charge gap in Refs. 11 and 20. It was shown that $2\Delta\rho \simeq 1/4(t_1+t_2)$, which provides $\Delta\rho \simeq 300$ K for $(\mathrm{TMTTF})_2\mathrm{PF}_6$. At the same time this magnitude of energy gap is two times smaller than the value reported in a previous publication.[2] This difference can be a result of the gap determination in Ref. 2 from $G(1/T)$ dependence obtained by averaging of $G(1/T)$ dependencies from several different samples with jumps of G due to cracks. The jumplike decrease of conduction at every crack results in more steep averaged $G(1/T)$ dependence and accordingly in more higher gap magnitude. The small cooling rate enables us to avoid cracks and to determine more accurately the energy-gap magnitude that agrees with theoretical evaluation.[11]

At lower temperature we observed a bend on the $G(1/T)$ dependence near $T_b = 70$ K, i.e., G begins to decrease more faster (activation energy ≈ 380 K) with a following gradual transition to a new activation regime at temperatures below 25 K. Detailed measurements of sample 2 show that the decrease of G is thermally activated between 4.2 and 20 K with an activation energy $\simeq 36$ K. This energy gap satisfied the BCS-like relation $\Delta = 1.75kT_{\mathrm{SP}}$ with $T_{\mathrm{SP}} \simeq 20$ K as previously shown in the temperature dependence of the electron paramagnetic resonance (EPR) spin susceptibility and the nuclear relaxation rate T_1^{-1}.[18]

It can also be seen in Fig. 1 that the frequency dependence of $G(1/T)$ becomes noticeable below 70 K with a frequency dispersion growing at lower temperature. For showing more precisely the particular points on the $G(1/T)$ variation, we draw in inset (b) of Fig. 1, the temperature variation of the logarithmic derivative that was reproducible for our three samples. The decrease of G near $T_b \simeq 70$ K may indicate the beginning of a transition into some new ground state.

The temperature variation of the real part of the dielectric permittivity $\epsilon'(T)$ of sample 1 in the frequency range 10^3–5×10^6 Hz is shown in Fig. 2. Between 300 and 220 K, the magnitude of ϵ' is below the background level determined by the resolution of our measurements in this temperature range. The growth of ϵ' is noticeable below $\simeq 200$ K and frequency independent down to $T \simeq 110$ K. Below this temperature a significant frequency dispersion occurs as seen in Fig. 2: at a given frequency, $\epsilon'(T)$ goes through a maximum before falling down. With decreasing frequency, the amplitude of the maximum of $\epsilon'(T)$ is larger

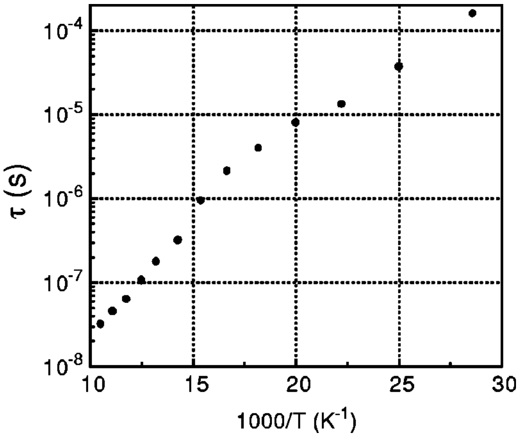

FIG. 3. Temperature dependence of the relaxation time τ of the dielectric relaxation (sample 1).

and the maximum position on the temperature scale shifts to lower temperature. This behavior is qualitatively similar to critical slowing down phenomena near a phase transition. The $\epsilon'(T)$ curves for samples 1 and 2 are shown in the inset of Fig. 2 in a double-logarithmic scale, manifesting their qualitative similarity. In the temperature range 200–70 K, the $\epsilon'(T)$ dependence can be described by the power law: $\epsilon'(T)\sim T^{-\alpha}$ with $\alpha\simeq 1/3$. While $\epsilon'(T)$ is decreasing from 70 down 10 K, a small bump in $\epsilon'(T)$ can be seen near $\simeq 35$ K.

The frequency dependencies of the conductance, of the real part ϵ', and of the imaginary part ϵ'' of the dielectric permittivity of $(\mathrm{TMTTF})_2\mathrm{PF}_6$ have a form similar to those we previously measured on other 1D organic compounds.[17,19] As usual, the frequency f_m corresponding to the maximum of $\epsilon''(T)$ corresponds to some mean value of the relaxation time $\tau = 1/2\pi f_m$ of charge polarization. The variation of τ with the inverse temperature is drawn in Fig. 3 for sample 1 in the temperature range 95–35 K: for 60 K $<T<$ 95 K, $\tau(1/T)$ is thermally activated with an energy activation of $\sim$650 K; but, at lower T, 35 K$<T<$60 K, the activation energy is smaller, $\approx$380 K, the same as the activation energy of the conductivity in the same temperature range.

III. DISCUSSION

As follows from published data[1,18] and from our experimental results, $(\mathrm{TMTTF})_2\mathrm{PF}_6$ can be characterized by two distinct energy scales: temperature $T_\rho = 250$ K corresponding to the conduction maximum and $T_{\mathrm{SP}}\simeq 20$ K corresponding to the transition into the spin-Peierls state. If one will consider the temperatures $T_{\mathrm{SP}}<T<T_\rho$ as a range of simple localization of charge carriers,[1] one could try to explain the observed growth of ϵ' as a result of the growth of $2k_F$ CDW fluctuations when approaching T_{SP}.[20] As was mentioned in Ref. 8, the temperature range of fluctuations near the spin-Peierls transition can be wide enough and reach $\sim 3T_{\mathrm{SP}}$. It means that in $(\mathrm{TMTTF})_2\mathrm{PF}_6$ the manifestation of the fluctuations can be noticed beginning from $T = T_{\mathrm{SP}} + 3\times T_{\mathrm{SP}} \simeq 80$ K, the temperature at which $2k_F$ fluctuations have started to be really observed.[20] However, as can be seen from Fig. 2, the ϵ' growth begins nevertheless not from 80 K but from $\simeq 200$ K. For frequencies above 10^6 Hz this ϵ' growth is rather achieved at 80 K. This dismatching in the temperature ranges for occurrence of $2k_F$ fluctuations and the ϵ' growth makes difficult the explanation of ϵ' growth as a result of $2k_F$ CDW fluctuations. In the same temperature range 50–200 K, EPR susceptibility χ decreases monotonously without any maximum.[18] A small maximum on $\chi(T)$ dependence was observed near 40 K with a following decrease of χ as a result of the transition to the spin-Peierls state. Such considerable qualitative difference between $\epsilon'(T)$ and $\chi(T)$ dependencies confirms the existence of spin-charge separation in $(\mathrm{TMTTF})_2\mathrm{PF}_6$ salts.

We tentatively ascribe the frequency and temperature dependencies of ϵ' of $(\mathrm{TMTTF})_2\mathrm{PF}_6$ in the temperature range $T_{\mathrm{SP}}<T<T_\rho$ as related to the charge induced correlation phenomena discussed above. Taking into account the dimerization and on-site interactions in the Hubbard model for the half-filled band, the commensurate charge induced superstructure is strictly linked to the host lattice. In such a case the possibility of polarization of the superstructure, i.e., its shift with respect to the host lattice, is small and consequently one would expect a low magnitude of the dielectric permittivity. The ground state with a Mott-Hubbard gap and appropriate charge localization have been realized in 3D semiconductors.[21] In such compounds ϵ' is of the order 10, a typical value for usual semiconductors, while in our samples of $(\mathrm{TMTTF})_2\mathrm{PF}_6$, the ϵ' magnitudes amount by several orders of value larger (Fig. 2).

As explained above, long-range Coulomb interaction of sufficient strength and appropriate charge induced correlation may lead to a superstructure with charge disproportionation corresponding to a $4k_F$ CDW as in a Wigner crystal. For $(\mathrm{TMTTF})_2\mathrm{PF}_6$ this charge disproportionation can be evaluated on the base of calculations in Ref. 13 taking into account the estimated magnitude of the reduced near-neighbor Coulomb interaction $V/t_2\simeq 2$.[4,12] For such a V/t_2 value we estimate the charge disproportionation as about 1:3.

The transition towards a new charge ordered state is characterized by a new order parameter and the opening of another energy gap. As is well known, more or less wide fluctuations may appear at temperatures near a phase transition. In this fluctuating temperature range the rigidity of the charge superstructure is reduced and consequently it becomes more easily polarizable. We ascribe the large magnitude of the dielectric permittivity that we have found, to the fluctuational collective response of such charge superstructure of Wigner crystal type with charge disproportionation formed in $(\mathrm{TMTTF})_2\mathrm{PF}_6$. Indeed, as can be seen from Fig. 2, in the temperature range above T_ρ, the ϵ' magnitude does not exceed the background level. Its noticeable growth begins below 200 K when, as we considered, the growing of this Wigner-type CDW superstructure begins to determine the kinetic properties of the compound. Near T_b a bump is visible in the temperature dependence of the conductivity (Fig. 1), which is a characteristic feature of a phase transition. The maximum value of ϵ' amounts to 10^5–10^6, two or three orders of magnitude lower than the ϵ' values in incommensurate charge[22] and spin[19] density wave below their transition temperature. However the magnitude of ϵ' in $(\mathrm{TMTTF})_2\mathrm{PF}_6$ is nearly comparable with that in $(\mathrm{TMTTF})_2\mathrm{Br}$.[17] The interpretation given in Ref. 17 for the temperature dependence of ϵ' of $(\mathrm{TMTTF})_2\mathrm{Br}$ would need to be reconsidered at the light of the present results showing charge ordering, a property that very likely is general for the whole family of $(\mathrm{TMTTF})_2\mathrm{X}$ compounds.

When the temperature is decreased below T_b, fluctuations also decrease but interchain correlations and interchain interactions increase. Both of them favor the three-dimensional ordering of a $4k_F$ CDW commensurate superstructure resulting in the decrease of the ϵ' magnitude. The slowing down behavior of ϵ' and the temperature depencence of the relaxation time [Fig. 3 also indicates the lattice involvement (i.e., heavy molecules) in the relaxation process].

According to x-ray measurements,[20] diffuse $2k_F$ scattering grows critically in $(\mathrm{TMTTF})_2\mathrm{PF}_6$ below ~ 70 K, which originates from the gradual enhancement of spin induced electron-electron correlation of antiferromagnetic type. Due to the growth of the electron-phonon interaction and of the increasing of the interchain interaction, these $2k_F$ spin induced correlations diverge below T_{SP} resulting in the condensation of an ordered spin-Peierls state with a $2k_F$ superstructure.

IV. CONCLUSION

In conclusion, our measurements of the complex conductivity of $(\mathrm{TMTTF})_2\mathrm{PF}_6$ show the main following features: (1) development of a charge energy gap the magnitude of which corresponds to theoretical evaluations in the frame of the extended Hubbard model; (2) existence of peculiarities on $G(1/T)$ dependence, for example, a minimum of the logarithmic derivative near 70 K; (3) in the same temperature range, finding of a huge maximum of the real part of the dielectric permittivity (up to 10^6) with a slowing down behavior with decreasing temperature while the magnetic susceptibility does not show any significant variation, which corresponds to large charge polarization simultaneously with spin-charge separation; and (4) considerable difference between the temperature dependence of the dielectric permittivity and $2k_F$ diffuse x-ray scattering.

All these features seem to confirm the possibility of the formation in the temperature range $T_{\mathrm{SP}} < T < T_\rho$ of a charge ordered state. On the basis of our experimental results and some theoretical approaches, we consider that the huge amplitude of the real part of the dielectric permittivity of $(\mathrm{TMTTF})_2\mathrm{PF}_6$ can hardly be provided by a Mott insulator. On the contrary, we argue that this large dielectric polarizability reflects the fluctuational collective response of the $4k_F$ charge-density wave of Wigner crystal type due to long-range Coulomb interaction and electron-electron correlation. Recently charge disproportionation[23] and $4k_F$ superlattice[24] have been reported from NMR and x-ray measurements in a 1/4-filled 1D organic compound $(\mathrm{DI\text{-}DCNQI})_2\mathrm{Ag}$ without dimerization.

ACKNOWLEDGMENTS

We would like to thank S. Brazovskii and N. Kirova for helpful discussions, and D. Staresinic for help in the experiment. Part of this work was supported by the Russian Fund for Fundamental Research (Grant No. 99-02-17364) and the twinning research programme No. 19 (Grant No. 98-02-22061) between CRTBT-CNRS and IRE-RAS.

---

[1] D. Jérome, Solid State Commun. **92**, 89 (1994); D. Jérome, P. Auban-Senzier, L. Balicas *et al.*, Synth. Met. **70**, 719 (1995).

[2] C. Coulon, P. Delhaes, S. Flandrois *et al.*, J. Phys. (France) **43**, 1059 (1982).

[3] R. Laversanne, C. Coulon, B. Gallois *et al.*, J. Phys. (France) Lett. **45**, L393 (1984).

[4] A. Fritsch and L. Ducasse, J. Phys. I **1**, 855 (1991); F. Castet, A. Fritsch, and L. Ducasse, *ibid.* **6**, 583 (1996).

[5] V.J. Emery, R. Bruisma, and S. Barisic, Phys. Rev. Lett. **48**, 1039 (1982).

[6] P.A. Lee, T.M. Rice, and R.A. Klemm, Phys. Rev. B **15**, 2984 (1977).

[7] S.K. Khanna, J.P. Pouget, R. Comes, A.F. Garito, and A.J. Heeger, Phys. Rev. B **16**, 1468 (1977); S. Kagoshima, T. Ishiguro, and H. Anzai, J. Phys. Soc. Jpn. **41**, 2061 (1976).

[8] H.J. Schulz, Int. J. Mod. Phys. B **5**, 57 (1991); in *Low-Dimensional Conductors and Superconductors*, edited by D. Jérome and L. Caron, NATO ASI Series B: Physics, Vol. 155, p. 95.

[9] J.E. Hirsch and D.J. Scalapino, Phys. Rev. B **27**, 7169 (1983); **29**, 5554 (1984).

[10] L.G. Caron and C. Bourbonnais, Phys. Rev. B **29**, 4230 (1984).

[11] K. Penc and F. Mila, J. Phys. IV **C2**, 155 (1991); Phys. Rev. B **50**, 11 429 (1994).

[12] F. Mila, Phys. Rev. B **52**, 4788 (1995).

[13] H. Seo and H. Fukuyama, J. Phys. Soc. Jpn. **66**, 1249 (1997).

[14] C. Bourbonnais, Synth. Met. **84**, 19 (1997); C. Bourbonnais and D. Jérome, in *Advances in Synthetic Metals*, edited by P. Bernier, S. Lefrant, and G. Bidan (Elsevier, Amsterdam, 1999), p. 206.

[15] R. Clay, A. Sandvic, and D. Campbell, Phys. Rev. **59**, 4665 (1999).

[16] P. Delhaes, C. Coulon, J. Amiell, S. Flandrois, E. Tororeilles, J.M. Fabre, and L. Giral, Mol. Cryst. Liq. Cryst. **50**, 43 (1979).

[17] F. Nad, P. Monceau, and J.M. Fabre, Eur. Phys. J. B **3**, 301 (1998).

[18] P. Wzietek, F. Creuzet, C. Bourbonnais, D. Jérome, K. Bechgaard, and P. Batail, J. Phys. I **3**, 171 (1993).

[19] F. Nad, P. Monceau, and K. Bechgaard, Solid State Commun. **95**, 655 (1995).

[20] J.P. Pouget and S. Ravy, J. Phys. I **6**, 1501 (1996); Synth. Met. **85**, 1523 (1997).

[21] N. F. Mott, *Metal-Isulator Transition* (Taylor and Francis, London, 1974).

[22] F. Nad and P. Monceau, Phys. Rev. B **51**, 2052 (1995).

[23] K. Hiraki and K. Kanada, Phys. Rev. Lett. **80**, 4737 (1998).

[24] Y. Nogami, K. Oshima, K. Hiraki, and K. Kanoda, J. Phys. IV **9**, 10 (1999).